Open charm effects in the explanation of the long-standing "$\rho\pi$ puzzle"

Qian Wang,[1] Gang Li,[3] and Qiang Zhao[1,2]

[1]*Institute of High Energy Physics, Chinese Academy of Sciences, Beijing 100049, People's Republic of China*
[2]*Theoretical Physics Center for Science Facilities, CAS, Beijing 100049, People's Republic of China*
[3]*Department of Physics, Qufu Normal University, Qufu, 273165, People's Republic of China*

(Received 9 January 2012; published 11 April 2012)

A detailed analysis of the open charm effects on the decays of $J/\psi(\psi') \to VP$ is presented, where V stands for light vector meson and P for light pseudoscalar meson. These are the channels that the so-called "12% rule" of perturbative QCD (pQCD) is obviously violated. Nevertheless, they are also the channels that violate the pQCD helicity selection rule at leading order. In this work, we put constraints on the electromagnetic contribution, short-distance contribution from the $c\bar{c}$ annihilation at the wave function origin, and long-distance contribution from the open charm threshold effects on these two decays. We show that interferences among these amplitudes, in particular, the destructive interferences between the short-distance and long-distance strong amplitudes, play a key role to evade the helicity selection rule and cause the significant deviations from the pQCD expected 12% rule.

DOI: 10.1103/PhysRevD.85.074015 PACS numbers: 13.25.Gv, 12.38.Lg, 12.40.Vv

I. INTRODUCTION

Annihilation decays of heavy quarkonium have served as an important probe for the study of the perturbative QCD (pQCD) strong interactions in the literature [1–3]. In the bottomonium energy region, the nonrelativistic approximation works well so that the annihilation of the $b\bar{b}$ can be regarded as a direct measurement of the properties of the bottomonium wave functions at the origin at leading order. For instance, for the S wave states, the annihilation matrix elements are proportional to the wave function at the origin, while for the P wave states to the first derivative at the origin. These simple relations have been broadly examined and found in good agreement with the experimental measurements in inclusive processes. They can be regarded as a direct test of the pQCD properties. Interestingly, although the mass of the charm quark cannot be regarded heavy enough, some of the leading pQCD relations are still well respected in inclusive transitions. A good example is the branching ratio fraction between ψ' and J/ψ:

$$R \equiv \frac{\mathrm{BR}(\psi' \to \mathrm{hadrons})}{\mathrm{BR}(J/\psi \to \mathrm{hadrons})} \simeq \frac{\mathrm{BR}(\psi' \to e^+e^-)}{\mathrm{BR}(J/\psi \to e^+e^-)} \simeq 0.13, \tag{1}$$

which is the so-called 12% rule and the branching ratio fractions probe the ratio of the wave functions at their origins for the ground state J/ψ and first radial excitation ψ'. Note that in the above equation both branching ratios $\mathrm{BR}(J/\psi \to \mathrm{hadrons})$ and $\mathrm{BR}(\psi' \to \mathrm{hadrons})$ are referred to their light hadron decays. In fact, even for some of those exclusive decays, the above relation seems to hold approximately well. Such an observation, in contrast with the significant deviations in J/ψ and $\psi' \to \rho\pi$, has initiated tremendous interests in the study of transition mechanisms for J/ψ and $\psi' \to \rho\pi$, which is known as the so-called "$\rho\pi$ puzzle." According to the Particle Data Group 2010 (PDG2010) [4], the ratio for the $\rho\pi$ channel is $\mathrm{BR}(\psi' \to \rho\pi)/\mathrm{BR}(J/\psi \to \rho\pi) \simeq (1.1 \sim 2.8) \times 10^{-3}$, which is much smaller than the pQCD expected value, i.e. $\sim$12%.

An alternative expression for the $\rho\pi$ puzzle is related to the power law suppression due to the pQCD helicity selection rule (HSR). As demonstrated in Refs. [2,3], the decay of $J/\psi(\psi') \to VP$, where V and P stand for vector and pseudoscalar meson, respectively, should be strongly suppressed at leading twist. As a consequence, the branching ratio fraction is expected to be $\mathrm{BR}(\psi' \to \rho\pi)/\mathrm{BR}(J/\psi \to \rho\pi) \simeq (M_{J/\psi}/M_{\psi'})^6 \times (\mathrm{BR}(\psi' \to \mathrm{hadrons})/\mathrm{BR}(J/\psi \to \mathrm{hadrons})) \sim 6.2\%$, which is still much larger than the experimental observations. The significant violation of the pQCD HSR is nontrivial taking into account that quite many exclusive decay channels have approximately respected the 12% rule.

Such a conflicting phenomenon has attracted a lot of attention from both experiment and theory in history. Even right now, the study of the $\rho\pi$ puzzle has been one of the most important physics goals in the program of BESIII experiment [5]. In theory, this puzzle has also been broadly studied. Different explanations have been proposed in the literature, such as the color-octet model [6], vector meson mixing [7,8], final-state interactions [9,10], admixtures of a vector glueball near J/ψ [11,12], intrinsic charm in light mesons [13], light-quark mixing effects [14], large survival decay of ψ' via virtual charmonium state [15], and interferences between the electromagnetic (EM) and strong interactions [16–19]. In the meantime, it has been realized that the $\rho\pi$ puzzle is not just restricted to the $\rho\pi$ decay channel. It has also connections with the obvious charge asymmetries observed in $\psi' \to K^*\bar{K} + c.c.$ Therefore, it was conjectured that more general dynamic reasons should be investigated for $J/\psi(\psi') \to VP$ [18,20–23].

It should be useful to recall the results of Ref. [18], where a global fit for $J/\psi(\psi') \to VP$ is presented. The EM and strong transition amplitudes are parameterized out for all the decay channels, while among the strong transition amplitudes, the singly disconnected OZI (SOZI) processes and doubly disconnected OZI (DOZI) processes are further parameterized out. As shown in Ref. [18], there exists an overall suppression on the strong decay amplitudes of $\psi' \to VP$, not just in the $\rho\pi$ channel. Because of this suppression, the EM transition amplitudes become compatible with the strong decay amplitudes with which the interferences produce further deviations from the HSR-violating power law suppressions. This fitting result at least clarifies the following two issues: (i)The same mechanism that suppresses $\psi' \to \rho\pi$ also plays a role in other $\psi' \to VP$ decays; and (ii) such a mechanism does not affect much in $J/\psi \to VP$ as suggested by the charge asymmetries observed in $K^*\bar{K} + c.c.$ These are important guides for exploring mechanisms that would suppress the strong decay amplitudes in $\psi' \to VP$, but have less impact on the J/ψ decays.

During the past few years, we have been focussing on the study of mechanisms evading the HSR in charmonium decays. For charmonia below the open $D\bar{D}$ threshold, the HSR-violating transitions are naturally correlated with the OZI-rule violations. As demonstrated in a series of studies [24–28], we have shown that the intermediate D meson loops (IMLs) provide a natural mechanism for evading the OZI rule and hence the HSR in charmonium decays. The IML is introduced as a nonperturbative source of contributions. As iterated in Refs. [20,21,24,25,29], apart from the $\rho\pi$ puzzle, the IML could be a key for understanding some of those long-standing questions in charmonium exclusive decays, e.g. the $\psi(3770)$ non-$D\bar{D}$ decay, large HSR-violating decay of $\eta_c \to VV$, M1 transition problems with $J/\psi(\psi') \to \gamma\eta_c(\eta_c')$, etc.

In this work, we provide a quantitative study of the role played by the long-distance IML in $J/\psi(\psi') \to VP$ in association with the EM and short-distance SOZI transitions. Our purpose is to demonstrate that the IMLs, as nonperturbative transition mechanisms, are important for explaining the phenomena observed in $J/\psi(\psi') \to VP$, and hence could be a natural solution for the long-standing $\rho\pi$ puzzle and other puzzles in charmonium exclusive decays. As follows, the details of dealing with different transition amplitudes are given in Sec. II. The numerical results and detailed analysis are presented in Sec. III, and a summary in the last section.

II. THE MODEL

A unique feature with the VVP coupling is that at hadronic level the antisymmetric tensor coupling is the only allowed Lorentz structure. Therefore, it can be understood that whatever the underlying mechanisms could be, they will contribute to the corrections to the antisymmetric tensor coupling. Based on this, one can always make a general parametrization to the transition amplitude,

$$\mathcal{M}_{\text{tot}} \equiv \mathcal{M}_{\text{EM}} + e^{i\delta_0}(\mathcal{M}_{\text{short}} + e^{i\theta}\mathcal{M}_{\text{long}}), \qquad (2)$$

where $\mathcal{M}_{\text{EM}}$, $\mathcal{M}_{\text{short}}$, and $\mathcal{M}_{\text{long}}$ are the amplitudes of the EM, strong short-distance, and strong long-distance transitions, respectively. A phase angle θ is introduced between the short- and long-distance amplitudes, while the relative phase between the EM and short-distance amplitudes is $\delta_0 = 0°$ or $180°$. It is reasonable to consider the trivial relative phase angles between the EM and short-distance amplitude. Meanwhile, the long-distance amplitude may carry a phase angle relative to the short-distance one due to hadronic wave function effects. Although the exclusive amplitudes for these three sources are obtained as real numbers, the relative phase angle θ can lead to a complex coupling in $J/\psi(\psi') \to VP$. We note that the EM amplitudes for each decay modes carry intrinsic signs deduced in the quark model [16]. Our efforts as follows are to constrain these amplitudes and present an overall prescription for $J/\psi(\psi') \to VP$.

A. EM transition amplitudes

The EM transition $J/\psi(\psi') \to \gamma^* \to VP$ turns out to be important in $J/\psi(\psi') \to VP$. In particular, it is the dominant contribution to those isospin-violating decay channels, i.e. $J/\psi(\psi') \to \rho\eta$, $\rho\eta'$, $\omega\pi^0$, and $\phi\pi^0$. This mechanism can be investigated in the vector meson dominance (VMD) model as presented in Refs. [18,19].

In Fig. 1 those three independent electromagnetic transition processes in the VMD are illustrated. The vertex couplings can be extracted from the experimental data for the decay widths of $V \to \gamma P$ (or $P \to \gamma V$), and $P \to \gamma\gamma$. However, since the intermediate photon is off-shell, a form factor $\mathcal{F}(q^2) = \Lambda_{\text{EM}}^2/(\Lambda_{\text{EM}}^2 - q^2)$ is adopted for the EM

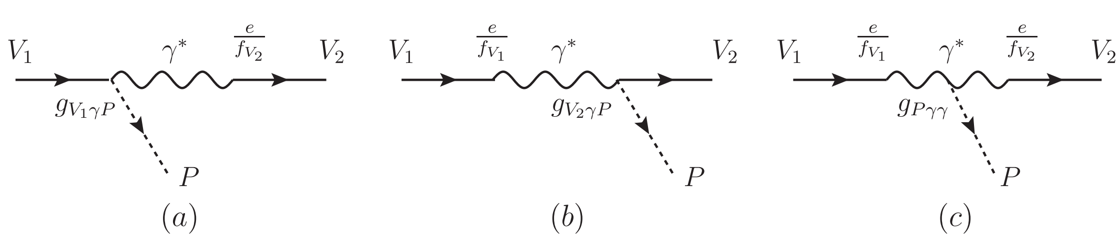

FIG. 1. The tree level Feynman diagrams of EM transitions in $J/\psi(\psi') \to VP$.

transition amplitudes. The cutoff energy Λ_{EM} is universal for both J/ψ and ψ' decays, and to be determined by experimental data for those isospin-violating decay channels. The EM amplitude can thus be expressed as

$$\mathcal{M}_{EM} = \mathcal{M}_a + \mathcal{M}_b + \mathcal{M}_c = \Big(\frac{e}{f_{V_2}}\frac{g_{V_1\gamma P}}{M_{V_1}}\mathcal{F}_a + \frac{e}{f_{V_1}}\frac{g_{V_2\gamma P}}{M_{V_2}}\mathcal{F}_b + \frac{e^2}{f_{V_1}f_{V_2}} \times \frac{g_{P\gamma\gamma}}{M_P}\mathcal{F}_c\Big)\epsilon_{\mu\nu\alpha\beta}p^\mu\epsilon(p)^\nu k^\alpha\epsilon(k)^\beta, \quad (3)$$

where $p(k)$ is the four momentum of the initial vector charmonium (final light vector), and $\epsilon(p)$ ($\epsilon(k)$) is its corresponding polarization vector. In Tables I, II, and III the EM vertex couplings are extracted with the up-to-date data from the PDG2010 [4].

B. Short-distance transition amplitudes

The short-distance contribution of strong interaction is mainly from the $c\bar{c}$ annihilation at the wave function origin associated with hard gluon radiations. This is an SOZI transition and can be parameterized out in a similar way as in Ref. [18]. We emphasize the $c\bar{c}$ annihilation at the wave function origin in this process. Thus, the HSR violation can be regarded as being produced by the non-negligible light-quark masses in the hadronization process. The inclusive gluon annihilation part is thus guaranteed to scale with their lepton pair branching ratio fraction since the inclusive amplitudes would be controlled by the quarkonium wave function at the origin [2]. This process distinguishes from the long-distance transitions via the IML where the $c\bar{c}$ annihilations would occur nonlocally and probe the charmonium wave function away from the origin. Such a difference would allow us to treat the short- and long-distance amplitudes individually and to avoid double counting between these two mechanisms. A schematic diagram for the short-distance SOZI transitions is shown in Fig. .

TABLE I. The couplings $g_{V\gamma P} \equiv [12\pi M_V^2\Gamma(V \to \gamma P)/|\mathbf{p}_\gamma|^3]^{1/2}$ or $g_{V\gamma P} \equiv [4\pi M_V^2\Gamma(P \to \gamma V)/|\mathbf{p}_\gamma|^3]^{1/2}$ determined by experimental data from PDG2010 [4].

$g_{V\gamma P}$	Values	Branching ratios
$g_{\rho\gamma\eta}$	0.381	$(3.00 \pm 0.20) \times 10^{-4}$
$g_{\rho\gamma\eta'}$	0.295	$(29.3 \pm 0.5)\%$
$g_{\rho^0\gamma\pi^0}$	0.196	$(6.0 \pm 0.8) \times 10^{-4}$
$g_{\rho^\pm\gamma\pi^\pm}$	0.170	$(4.5 \pm 0.5) \times 10^{-4}$
$g_{\omega\gamma\eta}$	0.107	$(4.6 \pm 0.4) \times 10^{-4}$
$g_{\omega\gamma\eta'}$	0.101	$(2.75 \pm 0.22)\%$
$g_{\omega\gamma\pi}$	0.545	$(8.28 \pm 0.28)\%$
$g_{\phi\gamma\eta}$	0.214	$(1.309 \pm 0.024)\%$
$g_{\phi\gamma\eta'}$	0.221	$(6.25 \pm 0.21) \times 10^{-5}$
$g_{\phi\gamma\pi}$	0.041	$(1.27 \pm 0.06) \times 10^{-3}$
$g_{K^{*\pm}\gamma K^\pm}$	0.226	$(9.9 \pm 0.9) \times 10^{-4}$
$g_{K^{*0}\gamma\bar{K}^0}$	0.344	$(2.39 \pm 0.21) \times 10^{-3}$
$g_{J/\psi\gamma\eta}$	3.31×10^{-3}	$(1.104 \pm 0.034) \times 10^{-3}$
$g_{J/\psi\gamma\eta'}$	8.04×10^{-3}	$(5.28 \pm 0.15) \times 10^{-3}$
$g_{J/\psi\gamma\pi}$	5.64×10^{-4}	$(3.49^{+0.33}_{-0.30}) \times 10^{-5}$
$g_{\psi'\gamma\eta}$	2.31×10^{-4}	$<2 \times 10^{-6}$
$g_{\psi'\gamma\eta'}$	1.93×10^{-3}	$(1.21 \pm 0.08) \times 10^{-4}$
$g_{\psi'\gamma\pi^0}$	3.534×10^{-4}	$<5.0 \times 10^{-6}$

TABLE II. The couplings $g_{P\gamma\gamma} \equiv (32\pi\Gamma(P \to \gamma\gamma)/M_P)^{1/2}$ determined by experimental data from PDG2010 [4].

$g_{P\gamma\gamma}$	Values	Γ_{tot}(keV)	Branching ratios
$g_{\pi\gamma\gamma}$	2.40×10^{-3}	7.86×10^{-3}	$(98.823 \pm 0.034)\%$
$g_{\eta\gamma\gamma}$	9.68×10^{-3}	1.3	$(39.31 \pm 0.20)\%$
$g_{\eta'\gamma\gamma}$	2.13×10^{-2}	194	$(2.22 \pm 0.08)\%$

TABLE III. The couplings $e/f_V \equiv [3\Gamma_{V\to e^+e^-}/(2\alpha_e|\mathbf{p}_e|)]^{1/2}$ determined by experimental data from PDG2010 [4].

e/f_V	Values($\times 10^{-2}$)	Γ_{tot}(MeV)	BR($V \to e^+e^-$)
e/f_ρ	6.11	149.1	$(4.72 \pm 0.05) \times 10^{-5}$
e/f_ω	1.80	8.49	$(7.28 \pm 0.14) \times 10^{-5}$
e/f_ϕ	2.25	4.26	$(2.954 \pm 0.03) \times 10^{-4}$
$e/f_{J/\psi}$	2.71	0.0929	$(5.94 \pm 0.06)\%$
$e/f_{\psi'}$	1.62	0.304	$(7.72 \pm 0.17) \times 10^{-3}$

The parametrization of the short-distance amplitudes is outlined as follows [18]. First, the strength of the nonstrange SOZI process is parameterized as

$$g_{J/\psi(\psi')} = \langle (q\bar{q})_V(q\bar{q})_P|V_0|J/\psi(\psi')\rangle, \quad (4)$$

where V_0 is the $3g$ decay potential of the charmonia into two nonstrange $q\bar{q}$ pairs of vectors and pseudoscalars via SOZI processes. It should be noted that the subscript V and P here do not mean that the quark-antiquark pairs are the SU(3) flavor eigenstates of vector and pseudoscalar mesons. The amplitude $g_{J/\psi(\psi')}$ is proportional to the charmonium wave functions at origin. Thus, it may have different values for J/ψ and ψ'.

Considering the SU(3) flavor symmetry breaking, which distinguishes the s quark pair production from the u, d quarks in the hadronizations, we introduce the SU(3) flavor symmetry breaking parameter ξ,

$$\xi \equiv \langle (q\bar{s})_V(s\bar{q})_P|V_0|J/\psi(\psi')\rangle/g_{J/\psi(\psi')} = \langle (s\bar{q})_V(q\bar{s})_P|V_0|J/\psi(\psi')\rangle/g_{J/\psi(\psi')}, \quad (5)$$

where $\xi = 1$ is in the SU(3) flavour symmetry limit, while deviations from unity implies the SU(3) flavor symmetry breaking. In general, the value of parameter ξ is around $\xi \simeq f_\pi/f_K = 0.838$, which provides a guidance for the SU(3) flavor symmetry breaking effects. For the production of two $s\bar{s}$ pairs via the SOZI potential, the recognition of the SU(3) flavor symmetry breaking in the transition is accordingly

$$\xi^2 = \langle (s\bar{s})_V (s\bar{s})_P | V_0 | J/\psi(\psi') \rangle / g_{J/\psi(\psi')}. \quad (6)$$

For the J/ψ and ψ' decays into isoscalar final states, such as $\omega\eta$, $\omega\eta'$, $\phi\eta$ and $\phi\eta'$, the DOZI transition as illustrated by Fig. may also contribute. Although it is not apparent that the DOZI transition can be classified as a short-distance process, we can parameterized it out as follows:

$$r \equiv \langle (q\bar{q})_V (q\bar{q})_P | V_1 | J/\psi(\psi') \rangle / g_{J/\psi(\psi')}, \quad (7)$$

where V_1 denotes the DOZI potential and a small value $|r| \ll 1$ would suggest a short-distance nature of this process. We mention that the DOZI process topologically does not double count the long-distance IML transitions to be defined in the next subsection.

To take into account the size effects of the initial- and final-state mesons, a commonly adopted form factor is included, i.e.

$$\mathcal{F}(\mathbf{P}) \equiv |\mathbf{P}|^l \exp(-\mathbf{P}^2/16\beta^2), \quad (8)$$

where $|\mathbf{P}|$ is the three-vector momentum of the final-state mesons in the $J/\psi(\psi')$ rest frame, and l is the final-state relative orbital angular momentum quantum number. We adopt $\beta = 0.5$ GeV, which is the same as Refs. [30–32]. At leading order the decays of $J/\psi(\psi') \to VP$ are via P-wave, i.e. $l = 1$.

The transition amplitudes for $J/\psi(\psi') \to VP$ via the short-distance SOZI transitions can then be expressed as

$$\begin{aligned}
\mathcal{M}_S(\rho^0\pi^0) &= \mathcal{M}_S(\rho^+\pi^-) = \mathcal{M}_S(\rho^-\pi^+) = g_{J/\psi(\psi')}\mathcal{F}(\mathbf{P}),\\
\mathcal{M}_S(K^{*+}K^-) &= \mathcal{M}_S(K^{*-}K^+) = \mathcal{M}_S(K^{*0}\bar{K}^0) = \mathcal{M}_S(\bar{K}^{*0}K^0) = g_{J/\psi(\psi')}\xi\mathcal{F}(\mathbf{P}),\\
\mathcal{M}_S(\omega\eta) &= X_\eta g_{J/\psi(\psi')}(1+2r)\mathcal{F}(\mathbf{P}) + Y_\eta\sqrt{2}\xi r g_{J/\psi(\psi')}\mathcal{F}(\mathbf{P}),\\
\mathcal{M}_S(\omega\eta') &= X_{\eta'} g_{J/\psi(\psi')}(1+2r)\mathcal{F}(\mathbf{P}) + Y_{\eta'}\sqrt{2}\xi r g_{J/\psi(\psi')}\mathcal{F}(\mathbf{P}),\\
\mathcal{M}_S(\phi\eta) &= X_\eta\sqrt{2}\xi r g_{J/\psi(\psi')}\mathcal{F}(\mathbf{P}) + Y_\eta g_{J/\psi(\psi')}(1+r)\xi^2\mathcal{F}(\mathbf{P}),\\
\mathcal{M}_S(\phi\eta') &= X_{\eta'}\sqrt{2}\xi r g_{J/\psi(\psi')}\mathcal{F}(\mathbf{P}) + Y_{\eta'} g_{J/\psi(\psi')}(1+r)\xi^2\mathcal{F}(\mathbf{P}),
\end{aligned} \quad (9)$$

where $X_\eta(X_{\eta'})$ and $Y_\eta(Y_{\eta'})$ are mixing amplitudes between $(u\bar{u}+d\bar{d})/\sqrt{2}$ and $s\bar{s}$ components within the η and η' wave functions

$$\begin{aligned}
\eta &= X_\eta|u\bar{u}+d\bar{d}\rangle/\sqrt{2} + Y_\eta|s\bar{s}\rangle,\\
\eta' &= X_{\eta'}|u\bar{u}+d\bar{d}\rangle/\sqrt{2} + Y_{\eta'}|s\bar{s}\rangle.
\end{aligned} \quad (10)$$

For the unitary 2×2 mixing, we have $X_\eta = Y_{\eta'} = \cos\alpha_P$ and $X_{\eta'} = -Y_\eta = \sin\alpha_P$ with $\alpha_P \equiv \theta_P + \arctan(\sqrt{2})$. The pseudoscalar mixing angle θ_P is in a range of $-22° \sim -13°$.

For the decays of $J/\psi(\psi') \to \rho\pi$ and $K^*\bar{K} + c.c.$, the short-distance amplitudes are rather simple as listed above. For the decays into isoscalar final states, the situation would be complicated by the DOZI process and glueball mixing. There have been a lot of studies of the glueball mixing in the η and η' wave function [18,33–35], which can contribute to the isoscalar decay channels. However, in this analysis we do not consider the glueball mixing effects since the glueball components within η and η' are rather small and need a delicate consideration. For the purpose of clarifying the role played by the short-distance and long-distance transition mechanisms in $J/\psi(\psi') \to VP$, we can leave the study of the glueball mixing effects to be considered in a differently motivated work [33].

C. Long-distance transition amplitudes via IML

The IML transitions as a nonperturbative process seem to be a natural mechanism to evade the OZI rule and HSR in the charmonium decays [24,25,27,28]. The relevant effective Lagrangians for the charmonium couplings to the charmed mesons are as the following [36,37]:

$$\mathcal{L} = i\frac{g_2}{2}\mathrm{Tr}[R_{c\bar{c}}\bar{H}_{2i}\gamma^\mu\overleftrightarrow{\partial}_\mu\bar{H}_{1i}] + \mathrm{H.c.}, \quad (11)$$

where the S-wave J/ψ and ψ' charmonium states are expressed as

$$R_{c\bar{c}} = \left(\frac{1+\not{v}}{2}\right)(\psi^\mu\gamma_\mu - \eta_c\gamma_5)\left(\frac{1-\not{v}}{2}\right). \quad (12)$$

The charmed and anticharmed meson triplet read

$$H_{1i} = \left(\frac{1+\not{v}}{2}\right)[\mathcal{D}_i^{*\mu}\gamma_\mu - \mathcal{D}_i\gamma_5], \quad (13)$$

$$H_{2i} = [\bar{\mathcal{D}}_i^{*\mu}\gamma_\mu - \bar{\mathcal{D}}_i\gamma_5]\left(\frac{1-\not{v}}{2}\right), \quad (14)$$

where $\mathcal{D}$ and $\mathcal{D}^*$ denote the pseudoscalar and vector charmed meson fields, respectively, i.e. $\mathcal{D}^{(*)} = (D^{0(*)}, D^{+(*)}, D_s^{+(*)})$.

Consequently, the Lagrangian for the S-wave J/ψ and ψ' is

$$\mathcal{L}_\psi = ig_{\psi\mathcal{D}^*\mathcal{D}^*}(g_{\mu\sigma}g_{\nu\rho} - g_{\mu\rho}g_{\nu\sigma} + g_{\mu\nu}g_{\rho\sigma})\psi^\mu \mathcal{D}^{*\nu}\overleftrightarrow{\partial}^\rho \mathcal{D}^{*\sigma\dagger} - ig_{\psi\mathcal{D}\mathcal{D}}\psi_\mu \mathcal{D}\overleftrightarrow{\partial}^\mu \mathcal{D}^\dagger - g_{\psi\mathcal{D}^*\mathcal{D}}\varepsilon^{\mu\nu\alpha\beta}\partial_\mu\psi_\nu(\mathcal{D}^*_\alpha\overleftrightarrow{\partial}_\beta\mathcal{D}^\dagger + \mathcal{D}\overleftrightarrow{\partial}_\alpha\mathcal{D}^{*\dagger}_\beta), \tag{15}$$

The Lagrangians relevant to the light vector and pseudoscalar mesons are,

$$\mathcal{L} = -ig_{\mathcal{D}^*\mathcal{D}\mathcal{P}}(\mathcal{D}^i\partial^\mu\mathcal{P}_{ij}\mathcal{D}^{*j\dagger}_\mu - \mathcal{D}^{*i}_\mu\partial^\mu\mathcal{P}_{ij}\mathcal{D}^{j\dagger}) + \tfrac{1}{2}g_{\mathcal{D}^*\mathcal{D}^*\mathcal{P}}\varepsilon_{\mu\nu\alpha\beta}\mathcal{D}^{*\mu}_i\partial^\nu\mathcal{P}^{ij}\overleftrightarrow{\partial}^\alpha\mathcal{D}^{*\beta\dagger}_j - ig_{\mathcal{D}\mathcal{D}\mathcal{V}}\mathcal{D}^\dagger_i\overleftrightarrow{\partial}_\mu\mathcal{D}^j(\mathcal{V}^\mu)^i_j - 2f_{\mathcal{D}^*\mathcal{D}\mathcal{V}}\epsilon_{\mu\nu\alpha\beta}(\partial^\mu V^\nu)^i_j(\mathcal{D}^\dagger_i\overleftrightarrow{\partial}^\alpha\mathcal{D}^{*\beta j} - \mathcal{D}^{*\beta\dagger}_i\overleftrightarrow{\partial}^\alpha\mathcal{D}^j) + ig_{\mathcal{D}^*\mathcal{D}^*\mathcal{V}}\mathcal{D}^{*\nu\dagger}_i\partial_\mu\mathcal{D}^{*j}_\nu(\mathcal{V}^\mu)^i_j + 4if_{\mathcal{D}^*\mathcal{D}^*\mathcal{V}}\mathcal{D}^{*\dagger}_{i\mu}(\partial^\mu\mathcal{V}^\nu - \partial^\nu\mathcal{V}^\mu)^i_j\mathcal{D}^{*j}_\nu, \tag{16}$$

with the convention $\varepsilon^{0123} = 1$, where $\mathcal{P}$ and $\mathcal{V}_\mu$ are 3×3 matrices for the octet pseudoscalar and nonet vector mesons, respectively,

$$\mathcal{P} = \begin{pmatrix} \frac{\pi^0}{\sqrt{2}} + \frac{\eta}{\sqrt{6}} & \pi^+ & K^+ \\ \pi^- & -\frac{\pi^0}{\sqrt{2}} + \frac{\eta}{\sqrt{6}} & K^0 \\ K^- & \bar{K}^0 & -\sqrt{\frac{2}{3}}\eta \end{pmatrix}, \qquad \mathcal{V} = \begin{pmatrix} \frac{\rho^0}{\sqrt{2}} + \frac{\omega}{\sqrt{2}} & \rho^+ & K^{*+} \\ \rho^- & -\frac{\rho^0}{\sqrt{2}} + \frac{\omega}{\sqrt{2}} & K^{*0} \\ K^{*-} & \bar{K}^{*0} & \phi \end{pmatrix}.$$

Based on the above Lagrangians, the explicit amplitudes in Fig. 3 can be obtained

$$\begin{aligned} M_{\mathcal{D}\bar{\mathcal{D}}\mathcal{D}^*} &= -4g_{\psi\mathcal{D}\mathcal{D}}g_{\mathcal{D}^*\mathcal{D}\mathcal{P}}f_{\mathcal{D}^*\mathcal{D}\mathcal{V}}\epsilon_\psi\cdot(p_2 - p_1)\epsilon_{\mu\nu\alpha\beta}p_2^\mu\epsilon^\nu p_3^\alpha q^\beta, \\ M_{\mathcal{D}\bar{\mathcal{D}}^*\mathcal{D}^*} &= -g_{\psi\mathcal{D}\mathcal{D}^*}g_{\mathcal{D}^*\mathcal{D}\mathcal{P}}\epsilon_{\mu\nu\rho\sigma}\epsilon^\mu_\psi p_1^\rho p_2^\sigma q^\lambda\left(-g_{\lambda\delta} + \frac{p_{3\lambda}p_{3\delta}}{m^2_{\mathcal{D}^*}}\right)(g_{\mathcal{D}^*\mathcal{D}^*\mathcal{V}}g^{\nu\delta}(p_2 - p_3)\cdot\epsilon - 4f_{\mathcal{D}^*\mathcal{D}^*\mathcal{V}}k^\delta\epsilon^\nu), \\ M_{\mathcal{D}^*\bar{\mathcal{D}}\mathcal{D}^*} &= -4g_{\psi\mathcal{D}^*\mathcal{D}}g_{\mathcal{D}^*\mathcal{D}^*\mathcal{P}}f_{\mathcal{D}^*\mathcal{D}^*\mathcal{V}}\epsilon_{\mu\rho\sigma\alpha}\epsilon^{\sigma\lambda\kappa\tau}\epsilon_{abc\tau}\epsilon^\mu_\psi p_1^\rho p_2^\alpha p_{1\lambda}p_{3\kappa}p_2^a\epsilon^b p_3^c, \\ M_{\mathcal{D}^*\bar{\mathcal{D}}\mathcal{D}} &= -g_{\psi\mathcal{D}^*\mathcal{D}}g_{\mathcal{D}^*\mathcal{D}\mathcal{P}}g_{\mathcal{D}\mathcal{D}\mathcal{V}}\epsilon_{\mu\rho\sigma\alpha}\epsilon^\mu_\psi p_1^\rho p_2^\alpha q^\sigma(p_2 - p_3)\cdot\epsilon, \\ M_{\mathcal{D}^*\mathcal{D}^*\mathcal{D}} &= -g_{\psi\mathcal{D}^*\mathcal{D}^*}g_{\mathcal{D}^*\mathcal{D}\mathcal{P}}f_{\mathcal{D}^*\mathcal{D}\mathcal{V}}\epsilon\epsilon_{\mu\nu\alpha\beta}p_3^\mu\epsilon^\nu p_2^\alpha q^\lambda\left(-g_{\lambda\delta} + \frac{p_{2\lambda}p_{2\delta}}{m^2_{\mathcal{D}^*}}\right) \\ &\quad\times(\epsilon^\delta_\psi(p_1 - p_2)^\beta - (p_1 - p_2)\cdot\epsilon g^{\delta\beta} + \epsilon^\beta_\psi(p_1 - p_2)^\delta), \\ M_{\mathcal{D}^*\bar{\mathcal{D}}^*\mathcal{D}^*} &= g_{\psi\mathcal{D}^*\mathcal{D}^*}g_{\mathcal{D}^*\mathcal{D}^*\mathcal{P}}\epsilon_{\mu\nu\alpha\alpha\beta}p_1^\nu p_3^\alpha(g_{\mathcal{D}^*\mathcal{D}^*\mathcal{V}}g^{\beta\lambda}(p_2 - p_3)\cdot\epsilon + 4f_{\mathcal{D}^*\mathcal{D}^*\mathcal{V}}k^\beta\epsilon^\lambda) \\ &\quad\times\left(-g_{\lambda\delta} + \frac{p_{2\lambda}p_{2\delta}}{m^2_{\mathcal{D}^*}}\right)(\epsilon^\mu_\psi(p_1 - p_2)^\delta - \epsilon\cdot(p_1 - p_2)g^{\mu\delta} + \epsilon(p_1 - p_2)^\mu), \end{aligned} \tag{17}$$

where p, k, q are the four-vector momenta of the incoming charmonium, outgoing light vector, outgoing pseudoscalar, respectively, and p_1, p_2, p_3 are the four-vector momenta of the intermediate charmed mesons as denoted in Fig. 3(a). The subscriptions in the amplitudes denote the intermediate charmed mesons in the loops, and we have omitted the denominators, form factors, and integral measurement $\int(d^4p_3)/(2\pi)^4$ to keep the formulas short. The following couplings are adopted in the numerical calculations [24,25,27,28]:

$$g_{\psi\mathcal{D}\mathcal{D}} = 2g_2\sqrt{m_\psi}m_\mathcal{D}, \quad g_{\psi\mathcal{D}\mathcal{D}^*} = \frac{g_{\psi\mathcal{D}\mathcal{D}}}{\tilde{M}_\mathcal{D}},$$
$$g_{\psi\mathcal{D}^*\mathcal{D}^*} = g_{\psi\mathcal{D}\mathcal{D}^*}\sqrt{\frac{m_{\mathcal{D}^*}}{m_\mathcal{D}}}m_{\mathcal{D}^*}, \quad \tilde{M}_\mathcal{D} = \sqrt{m_\mathcal{D}m_{\mathcal{D}^*}}, \tag{18}$$

where $g_2 = (\sqrt{m_\psi})/(2m_\mathcal{D}f_\psi)$, and m_ψ and $f_\psi = 405$ MeV are the mass and decay constant of J/ψ. The relative coupling strength of ψ' to J/ψ, i.e. $g_{\psi'\mathcal{D}\bar{\mathcal{D}}}/g_{J/\psi\mathcal{D}\bar{\mathcal{D}}} = 1$, is included as a input. The light meson couplings to the charmed mesons are [38]

$$g_{\mathcal{D}^*\mathcal{D}\mathcal{P}} = \frac{2g}{f_\pi}\sqrt{m_\mathcal{D}m_{\mathcal{D}^*}}, \quad g_{\mathcal{D}^*\mathcal{D}^*\mathcal{P}} = \frac{g_{\mathcal{D}^*\mathcal{D}\mathcal{P}}}{\sqrt{m_\mathcal{D}m^*_\mathcal{D}}},$$
$$g_{\mathcal{D}\mathcal{D}\mathcal{V}} = g_{\mathcal{D}^*\mathcal{D}^*\mathcal{V}} = \frac{\beta_0 g_\mathcal{V}}{\sqrt{2}}, \quad f_{\mathcal{D}^*\mathcal{D}\mathcal{V}} = \frac{f_{\mathcal{D}^*\mathcal{D}^*\mathcal{V}}}{m_{\mathcal{D}^*}} = \frac{\lambda g_\mathcal{V}}{\sqrt{2}},$$
$$g_\mathcal{V} = \frac{m_\rho}{f_\pi}, \tag{19}$$

where $g = 0.59$, $\beta_0 = 0.9$, $\lambda = 0.56\ \mathrm{GeV}^{-1}$, and $f_\pi = 132$ MeV are adopted.

The explicit amplitudes with different quantum number exchanges in the loops have been given in Eq. (17). For each decay mode the amplitude is dependent on the flavor component of the final-state light mesons. Thus, it is convenient to express the flavor-dependent amplitudes as

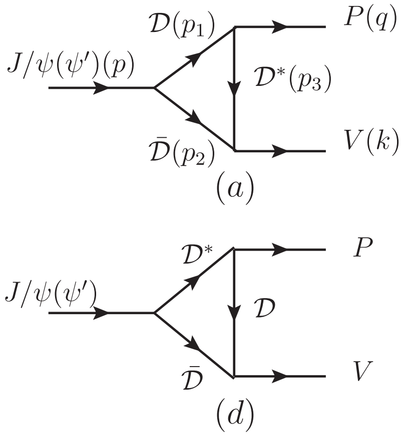

FIG. 3. Schematic diagrams for the long-distance IML transitions in $J/\psi(\psi') \to VP$. In this case, the c and $\bar{c}$ annihilate by multisoft-gluon radiations and can be described by intermediate charmed meson exchanges. The notations are $\mathcal{D} = (D^0, D^+, D_s^+)$ and $\bar{\mathcal{D}} = (\bar{D}^0, D^-, D_s^-)$. The light flavors of the charmed mesons are implicated by the final-state light mesons as shown in Eq. (20).

$$\begin{aligned}
\mathcal{M}_{\rho\eta} &= X_\eta \tfrac{1}{2}([\mathcal{D}^0\bar{\mathcal{D}}^0\mathcal{D}^0] - [\mathcal{D}^+\mathcal{D}^+\mathcal{D}^-]) + c.c.,\\
\mathcal{M}_{\rho\eta'} &= X_{\eta'} \tfrac{1}{2}([\mathcal{D}^0\bar{\mathcal{D}}^0\mathcal{D}^0] - [\mathcal{D}^+\mathcal{D}^+\mathcal{D}^-]) + c.c.,\\
\mathcal{M}_{\omega\pi^0} &= \tfrac{1}{2}([\mathcal{D}^0\bar{\mathcal{D}}^0\mathcal{D}^0] - [\mathcal{D}^+\mathcal{D}^+\mathcal{D}^-]) + c.c.,\\
\mathcal{M}_{\phi\pi^0} &= 0,\\
\mathcal{M}_{\rho^0\pi^0} &= \tfrac{1}{2}([\mathcal{D}^0\bar{\mathcal{D}}^0\mathcal{D}^0] + [\mathcal{D}^+\mathcal{D}^+\mathcal{D}^-]) + c.c.,\\
\mathcal{M}_{\rho^+\pi^-} &= [\mathcal{D}^0\bar{\mathcal{D}}^0\mathcal{D}^+ + \mathcal{D}^-\mathcal{D}^+\bar{\mathcal{D}}^0],\\
\mathcal{M}_{\omega\eta} &= X_\eta \tfrac{1}{2}([\mathcal{D}^0\bar{\mathcal{D}}^0\mathcal{D}^0] + [\mathcal{D}^+\mathcal{D}^+\mathcal{D}^-]) + c.c.,\\
\mathcal{M}_{\omega\eta'} &= X_{\eta'} \tfrac{1}{2}([\mathcal{D}^0\bar{\mathcal{D}}^0\mathcal{D}^0] + [\mathcal{D}^+\mathcal{D}^+\mathcal{D}^-]) + c.c.,\\
\mathcal{M}_{\phi\eta} &= Y_\eta[\mathcal{D}_s^+\mathcal{D}_s^-\mathcal{D}_s^+] + c.c.,\\
\mathcal{M}_{\phi\eta'} &= Y_{\eta'}[\mathcal{D}_s^+\mathcal{D}_s^-\mathcal{D}_s^+] + c.c.,\\
\mathcal{M}_{K^{*+}K^-} &= [\mathcal{D}_s^-\mathcal{D}_s^+\bar{\mathcal{D}}^0] + [\mathcal{D}^0\bar{\mathcal{D}}^0\mathcal{D}_s^+],\\
\mathcal{M}_{K^{*0}\bar{K}^0} &= [\mathcal{D}_s^-\mathcal{D}_s^+\mathcal{D}^-] + [\mathcal{D}^+\mathcal{D}^-\mathcal{D}_s^+],
\end{aligned} \tag{20}$$

where X_η ($X_{\eta'}$) and Y_η ($Y_{\eta'}$) have been defined earlier, and the amplitudes of $\rho^-\pi^+$, $K^{*-}K^+$ and $\bar{K}^{*0}K^0$ have been implicated by their conjugation channels listed above. Note that the destructive sign between the charged and neutral meson loop amplitudes in those isospin-violating channels, such as $\rho\eta$, $\rho\eta'$, $\omega\pi^0$. The IML amplitudes for the $\phi\pi^0$ channel vanish in the SU(3) symmetry limit.

Since the IML integrals are ultraviolet divergent, an empirical trimonopole form factor is introduced,

$$\mathcal{F} = \prod_i \frac{\Lambda_i^2 - m_i^2}{\Lambda_i^2 - p_i^2}, \tag{21}$$

where m_i is the mass of the exchanged particles and p_i is the corresponding four-vector momentum. As usual, Λ_i is parameterized into $\Lambda_i = m_i + \alpha\Lambda_{\rm QCD}$ with $\Lambda_{\rm QCD} =$ 0.22 GeV denoting the typical low energy scale of QCD.

III. MODEL RESULTS

A. Analyzing scheme

As mentioned earlier, all the underlying mechanisms in the VVP transitions would just contribute to the effective coupling constant. This feature, on the one hand, can provide advantages for disentangling different mechanisms, but on the other hand, may bring difficulties to the numerical fittings since the final results would only depend on the modulus of the summed amplitudes. Fortunately, the dynamic features of those different transition mechanisms as described in the previous section are useful for working out the parameter fitting scheme and disentangling the underlying mechanisms step by step. In Fig. 4, we illustrate the relation between the EM and strong transition amplitudes (including the short- and long-distance ones) by the addition of vectors in the complex plane. Our strategy of determining the amplitudes of those three transition processes is as follows:

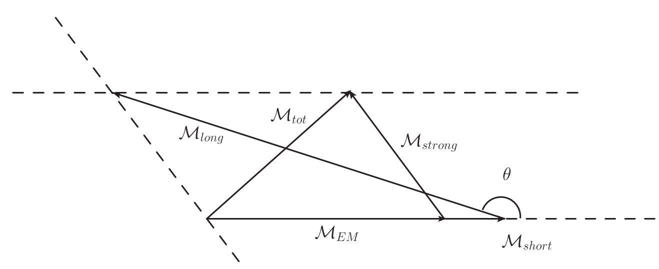

FIG. 4. Decomposition of the transition amplitudes for $J/\psi(\psi') \to VP$ in a complex plane. The EM amplitude is assigned to point to the real axis while the short-distance amplitude carries a trivial sign difference to the EM one. The long-distance IML amplitude carries a phase due to hadronic effects. The final summed amplitude $\mathcal{M}_{\rm tot}$ is to be compared with the experimental data.

(i) We treat the EM amplitude of each decay channel as a fixed vector in the complex plane pointing to the real axis as shown by Fig. 4.
The EM amplitudes can be independently fixed by the data for those isospin-violating channels, i.e. $J/\psi(\psi') \to \rho\eta$, $\rho\eta'$, $\omega\pi^0$ and $\phi\pi^0$. The same parameter $\Lambda_{\rm EM} = 0.542$ GeV are then adopted for other decay channels as a reliable estimate of the EM amplitudes in the VMD model [18].
It should be noted that as discussed in Ref. [18], the branching ratio fractions between ψ' and J/ψ decays into these isospin-violating channels are approximately within the range of 12% rule. This is an indication that for a single mechanism-dominant process, the branching ratio fractions still serves as a probe for the wave function at the origin. In another words, if other mechanisms play a role, interferences among those processes would break down the pQCD relation. Such a scenario would be a natural explanation for the deviations observed in other channels. For instance, in the $\rho\pi$ channel the interferences between the EM and strong amplitudes would lead to significant deviations from the 12% rule. Our focus in this work is to understand why the strong amplitude becomes compatible with the EM one in such an HSR-violating channel.

(ii) For the strong amplitudes including the short-distance and long-distance IML amplitudes, it is reasonable to impose that the EM and short-distance amplitude have a trivial relative phase since both probe the charmonium wave functions at the origin and both are real numbers. Moreover, for the short-distance SOZI amplitudes, we impose a constraint to require that their exclusive contributions should respect the 12% rule, i.e. the magnitude of the short-distance amplitudes can be treated as an input. Equation (2) can be rewritten as

$$\mathcal{M}_{\rm tot} \equiv \mathcal{M}_{\rm EM} + e^{i\delta}\mathcal{M}_{\rm strong}, \tag{22}$$

where $\mathcal{M}_{\rm strong}$ is the amplitude for the total strong transitions with a relative phase angle δ relative to the EM one. By an overall fit of the experimental data [18], the values of $\mathcal{M}_{\rm strong}$ and δ can be fixed for each channel. Then, with the fixed magnitude and direction for the EM and short-distance amplitudes, the decomposition of Eq. (22) will allow us to determine the magnitude and direction of the long-distance amplitude as shown by Fig. 4.
We note that the overall fit of phase angle δ in Ref. [18] suggests that all the VP channels in J/ψ or ψ' decays share the same value of δ. A consequence of such an implication is a constraint on the magnitude and direction for the long-distance amplitudes in each VP channel. What we are going to examine in the following part is the range of the form factor parameter α in the meson loops, namely, whether all the VP channels share the same value of α at all. The confirmation of such a scenario should be evidence for the important contributions from the IML in J/ψ and ψ' decays.
Following the above procedure, we first consider $\rho\pi$ and $K^*\bar{K} + c.c.$ decay channels. Since the final-state light mesons in these channels carry nonzero isospin, the short-distance transitions can only occur via the SOZI process while the DOZI process is forbidden. The analysis of these channels will then be able to expose the interfering feature of the IML.

B. Parameters and results

The parameters to appear in the analysis include the following: (i) The universal EM cutoff energy $\Lambda_{\rm EM} = 0.542$ GeV determined by the isospin-violating channels. (ii) The short-distance transition strength $g_{J/\psi} = 1.75 \times 10^{-2}$ in the J/ψ decay. This is an input for the short-distance amplitudes. It determines the short-distance transition strength $g_{\psi'} = 1.25 \times 10^{-2}$. Therefore, the exclusive contributions from the short-distance transitions still respect the 12% rule. (iii) The form factor parameters $\alpha_{J/\psi}$ and $\alpha_{\psi'}$ for the IML transitions which determine the long-distance coupling strengths. (iv) The phase angles $\theta_{J/\psi}$ and $\theta_{\psi'}$ between the EM and strong amplitudes in the J/ψ and ψ' decays, respectively, as defined in Eq. (22).

Other implicated parameters such as the SU(3) flavor symmetry breaking parameter $\xi = f_\pi/f_K \simeq 0.838$, vertex coupling constants for the IML in Sec. II C, and flavor mixing angle $\theta_P = -22°$ for η and η', in principle, have been determined by independent processes.

In Table IV, parameters adopted in the calculations are listed. As described in the above, some of those are treated as input, while the three parameters, i.e. the IML form factor parameter α, phase angle θ, and SU(3) flavor symmetry parameter ξ, are fitted by the experimental data for J/ψ and $\psi' \to \rho\pi$ and $K^*\bar{K} + c.c.$, respectively. When the isospin zero decay channels are included, such as J/ψ and $\psi' \to \omega\eta$, $\omega\eta'$, etc., the DOZI parameter r can also be fitted. We also list the χ^2 for the J/ψ and ψ' decays, respectively. Briefly speaking, with the small number of parameters, we can achieve a reasonable description of the

TABLE IV. Parameters fitted, respectively, by experimental data for J/ψ and $\psi' \to VP$ in our analysis scheme.

Parameter	J/ψ	ψ'
ξ	0.71 ± 0.017	0.92 ± 0.053
r	-0.201 ± 0.006	-0.097 ± 0.024
θ	$45.0° \pm 7.0°$	$174.6° \pm 2.9°$
α	0.09 ± 0.03	0.35 ± 0.01
χ^2	52.2	9.17

TABLE V. The effective couplings (in unit of GeV^{-1}) extracted from different transition mechanisms in $J/\psi(\psi') \to \rho\pi$ and $K^*\bar{K} + c.c.$

$J/\psi \to VP$	g_{EM}	g_{short}	g_{long}	$\lvert g_{\mathrm{strong}}\rvert$	$\lvert g_{\mathrm{tot}}\rvert$
$\rho^0\pi^0$	-2.26×10^{-4}	-2.36×10^{-3}	-1.60×10^{-5}	2.37×10^{-3}	2.60×10^{-3}
$K^{*+}K^-$	-2.17×10^{-4}	-1.78×10^{-3}	-1.45×10^{-5}	1.79×10^{-3}	2.0×10^{-3}
$K^{*0}\bar{K}^0$	3.28×10^{-4}	-1.78×10^{-3}	-1.45×10^{-5}	1.79×10^{-3}	1.46×10^{-3}
$\psi' \to VP$					
$\rho^0\pi^0$	-9.58×10^{-5}	-1.11×10^{-3}	-1.29×10^{-3}	2.11×10^{-4}	1.43×10^{-4}
$K^{*+}K^-$	-9.07×10^{-5}	-1.07×10^{-3}	-1.25×10^{-3}	2.07×10^{-4}	1.41×10^{-4}
$K^{*0}\bar{K}^0$	1.37×10^{-4}	-1.07×10^{-3}	-1.28×10^{-3}	2.33×10^{-4}	3.58×10^{-4}

overall experimental data, and the parameter uncertainties have been well constrained. The relatively large χ^2 value for the J/ψ decays are due to the relatively small experimental errors in this channel. One notices that the value of $\alpha_{J/\psi}$ has relatively large uncertainties in comparison with that of the $\alpha_{\psi'}$. This is because the IML contributions are relatively small in the J/ψ decays, and insensitive to the form factor parameter.

1. Isospin nonzero channels

In Table V, the effective couplings extracted from different transition mechanisms in J/ψ and $\psi' \to \rho\pi$ and $K^*\bar{K} + c.c.$ are listed. Comparing the coupling g_{short} in these two channels, one notices that the SU(3) flavor symmetry breaking is at the scale of $\xi = 0.71 \sim 0.92$ which is compatible with $\xi = f_\pi/f_K \simeq 0.838$. It shows that a small long-distance contribution from the IML will optimize the description of the data. The fitted form factor parameter $\alpha_{J/\psi} \simeq 0.09$ is adopted for all exclusive decay channels, which suggests a universal role played by the IML in $J/\psi \to VP$. The small contribution from the IML is understandable since the mass of J/ψ is much below the open charm threshold. Therefore, it does not experience the long-distance IML effects in the transition.

In $J/\psi \to VP$, the relatively small EM amplitudes implies insignificant interferences between the EM and strong transition amplitudes. This feature is indicated by the relatively small charge asymmetries between $J/\psi \to K^{*+}K^- + c.c.$ and $J/\psi \to K^{*0}\bar{K}^0 + c.c.$

For $\psi' \to VP$, the short-distance coupling strength is determined by the 12% rule relation. A proper description of the data leads to the determination of the long-distance IML amplitudes as listed in Table V. Since the mass of the ψ' is much closer to the open charm threshold, the long-distance IML amplitudes become sizeable and play an important role in $\psi' \to VP$. Given that the IML amplitudes are compatible with the short-distance ones in magnitude, the destructive interferences between the short and long-distance strong amplitudes have thus significantly lowered the strong transition amplitudes to be compatible with the EM ones. As a consequence, the further interferences with the EM amplitudes lead to the significant charge asymmetries between the branching ratios of $\psi' \to K^{*0}\bar{K}^0 + c.c.$ and $\psi' \to K^{*+}K^- + c.c.$

2. Isospin zero channels

For the isospin zero decay channels, such as $J/\psi(\psi') \to \omega\eta$, $\omega\eta'$, $\phi\eta$, and $\phi\eta'$, the DOZI transitions may contribute and two additional parameters have to be included [18]. One is the η-η' mixing angle α_P defined in Eq. (10) and the other is the DOZI coupling strength r defined in Eq. (7). We adopt the commonly used value $\alpha_P = 32.7°$ as an input, while treat r as a free parameter to be determined by the isospin zero decay channels. Meanwhile, all the other parameters determined in $J/\psi(\psi') \to \rho\pi$ and $K^*\bar{K} + c.c.$ are fixed.

Eventually, it cannot be regarded as an overall fitting, and we do not expect a perfect description of the data for $J/\psi(\psi') \to \omega\eta$, $\omega\eta'$, $\phi\eta$, and $\phi\eta'$. This is mainly because the involvement of the DOZI mechanism and possible glueball mixing in the isospin zero channels should be considered in a more delicate way. Therefore, we only expect that those isospin zero channels to be described to the correct order of magnitude.

In Table VI, the model calculations of the branching ratios of J/ψ and $\psi' \to VP$ are listed in comparison with the experimental values. The exclusive contributions from the EM, short-distance and long-distance IML transitions, and the combined strong contributions are also shown. The following points can be learned:

(i) For the isospin-violating channels, i.e. $J/\psi(\psi') \to \rho\eta$, $\rho\eta'$, etc., the charged and neutral meson loops would cancel out exactly in the isospin symmetry limit. In other words, because of the isospin symmetry breaking, the mass difference between the u and d quark leads to $m_{\mathcal{D}}^{(*)\pm} \neq m_{\mathcal{D}}^{(*)0}$. As a result, the charged and neutral meson loops cannot completely cancel out, and the residue part will contribute to the isospin-violating amplitudes. Interestingly, we find that contributions from such a mechanism is much smaller than the EM transitions, which makes the isospin-violating channels ideal for the test of the 12% rule. In Table VII, the branching ratio fraction R is listed for all the VP channels. One can see that the

TABLE VI. Theoretical results for the branching ratios of $J/\psi(\psi') \to VP$ calculated in our model. The experimental data are from PDG2010 [4].

$\mathrm{BR}(J/\psi \to VP)$	EM	Short distance	Long distance	Strong	Total	Experimental data
$\rho\eta$	1.81×10^{-4}	0	2.34×10^{-12}	2.34×10^{-12}	1.81×10^{-4}	$(1.93 \pm 0.23) \times 10^{-4}$
$\rho\eta'$	1.37×10^{-4}	0	2.21×10^{-12}	2.21×10^{-12}	1.37×10^{-4}	$(1.05 \pm 0.18) \times 10^{-4}$
$\omega\pi^0$	3.1×10^{-4}	0	2.38×10^{-12}	2.38×10^{-12}	3.10×10^{-4}	$(4.5 \pm 0.5) \times 10^{-4}$
$\phi\pi^0$	9.52×10^{-7}	0	0	0	9.52×10^{-7}	$<6.4 \times 10^{-6}$
$\rho^0\pi^0$	4.44×10^{-5}	4.85×10^{-3}	2.24×10^{-7}	4.89×10^{-3}	5.87×10^{-3}	$(5.6 \pm 0.7) \times 10^{-3}$
$\rho\pi$	1.06×10^{-4}	1.45×10^{-2}	6.71×10^{-7}	1.47×10^{-2}	1.73×10^{-2}	$(1.69 \pm 0.15) \times 10^{-2}$
$K^{*+}K^- + c.c.$	6.97×10^{-5}	4.69×10^{-3}	3.14×10^{-7}	4.74×10^{-3}	5.96×10^{-3}	$(5.12 \pm 0.3) \times 10^{-3}$
$K^{*0}\bar{K}^0 + c.c.$	1.59×10^{-4}	4.68×10^{-3}	3.11×10^{-7}	4.73×10^{-3}	3.16×10^{-3}	$(4.39 \pm 0.31) \times 10^{-3}$
$\omega\eta$	1.4×10^{-5}	1.76×10^{-3}	1.50×10^{-7}	1.78×10^{-3}	2.11×10^{-3}	$(1.74 \pm 0.20) \times 10^{-3}$
$\omega\eta'$	1.4×10^{-5}	9.91×10^{-5}	5.42×10^{-8}	1.02×10^{-4}	1.92×10^{-4}	$(1.82 \pm 0.21) \times 10^{-4}$
$\phi\eta$	2.35×10^{-5}	6.70×10^{-4}	3.22×10^{-8}	6.76×10^{-4}	9.52×10^{-4}	$(7.5 \pm 0.8) \times 10^{-4}$
$\phi\eta'$	2.10×10^{-5}	2.07×10^{-4}	6.45×10^{-8}	2.12×10^{-4}	9.93×10^{-5}	$(4.0 \pm 0.7) \times 10^{-4}$
$\mathrm{BR}(\psi' \to VP)$						
$\rho\eta$	1.42×10^{-5}	0	4.13×10^{-7}	4.13×10^{-7}	1.94×10^{-5}	$(2.2 \pm 0.6) \times 10^{-5}$
$\rho\eta'$	1.04×10^{-5}	0	3.89×10^{-7}	3.89×10^{-7}	1.48×10^{-5}	$(1.9^{+1.7}_{-1.2}) \times 10^{-5}$
$\omega\pi^0$	2.98×10^{-5}	0	4.25×10^{-7}	4.25×10^{-7}	3.73×10^{-5}	$(2.1 \pm 0.6) \times 10^{-5}$
$\phi\pi^0$	9.78×10^{-8}	0	0	0	9.78×10^{-8}	$<4.0 \times 10^{-6}$
$\rho^0\pi^0$	4.36×10^{-6}	5.81×10^{-4}	7.85×10^{-4}	2.12×10^{-5}	9.72×10^{-6}	***
$\rho\pi$	1.02×10^{-5}	1.74×10^{-3}	2.36×10^{-3}	6.36×10^{-5}	3.20×10^{-5}	$(3.2 \pm 1.2) \times 10^{-5}$
$K^{*+}K^- + c.c.$	7.03×10^{-6}	9.81×10^{-4}	1.33×10^{-3}	3.64×10^{-5}	1.70×10^{-5}	$(1.7^{+0.8}_{-0.7}) \times 10^{-5}$
$K^{*0}\bar{K}^0 + c.c.$	1.61×10^{-5}	9.81×10^{-4}	1.39×10^{-3}	4.61×10^{-5}	1.09×10^{-4}	$(1.09 \pm 0.20) \times 10^{-4}$
$\omega\eta$	1.10×10^{-6}	3.24×10^{-4}	5.57×10^{-4}	3.52×10^{-5}	2.48×10^{-5}	$<1.1 \times 10^{-5}$
$\omega\eta'$	1.12×10^{-6}	6.23×10^{-5}	2.31×10^{-4}	5.43×10^{-5}	4.01×10^{-5}	$(3.2^{+2.5}_{-2.1}) \times 10^{-5}$
$\phi\eta$	2.26×10^{-6}	1.55×10^{-4}	1.73×10^{-4}	1.92×10^{-6}	2.25×10^{-6}	$(2.8^{+1.0}_{-0.8}) \times 10^{-5}$
$\phi\eta'$	2.22×10^{-6}	1.85×10^{-4}	3.99×10^{-4}	4.33×10^{-5}	6.42×10^{-5}	$(3.1 \pm 1.6) \times 10^{-5}$

12% rule is reasonably respected in those isospin-violating channels.

(ii) For the final-state isospin nonzero channels, the systematic feature is that the long-distance amplitudes in $J/\psi \to \rho\pi$ and $K^*\bar{K} + c.c.$, are negligibly small and the strong amplitudes are dominated by the short-distance ones. In contrast, the strong amplitudes are suppressed in $\psi' \to \rho\pi$ and $K^*\bar{K} + c.c.$ because of the destructive cancellations between the short and long-distance amplitudes and become compatible with the EM ones. The observed branching ratio fractions are then further deviated from the 12% rule by the interferences between the EM and suppressed strong transition amplitudes in the ψ' decays. We have shown that the suppression of the strong amplitudes is due to the open charm threshold effects via the IML transitions. The branching ratio fraction R is also listed in Table VII to compare with the data. Moreover, with the exclusive short-distance transition satisfying the 12% rule in the $\rho\pi$ channel as a condition, other exclusive short-distance contributions also satisfy it fairly well.

(iii) For the final-state isospin zero channels, i.e. $J/\psi(\psi') \to \omega\eta$ and $\omega\eta'$, etc., the experimental data have relatively large uncertainties and can be accounted for approximately to the same order of magnitude. Similar to the study of Ref. [18], the DOZI contributions are found necessary. In this analysis we do not consider the glueball mixing

TABLE VII. The branching ratio fraction $R = \mathrm{BR}(\psi' \to VP)/\mathrm{BR}(J/\psi \to VP)$ given by our model (total) and the exclusive short-distance transitions. For the isospin-violating channels, the ratios are dominated by the EM transitions. The center dots indicated the transition is either absent or the data are not available. The experimental ratios are listed as a comparison.

VP mode (%)	$\rho\eta$	$\rho\eta'$	$\omega\pi^0$	$\phi\pi^0$	$\rho^0\pi^0$	$\rho\pi$	$K^{*+}K^- + c.c.$	$K^{*0}\bar{K}^0 + c.c.$.	$\omega\eta$	$\omega\eta'$	$\phi\eta$	$\phi\eta'$
Short distance	...	...	...	...	11.98	12.0	20.92	20.96	18.41	62.87	23.13	89.37
Total	10.72	10.80	12.03	10.27	0.17	0.18	0.29	3.45	1.18	20.89	0.24	64.65
Experiment	7.40	5.69	3.0	...	...	0.11	0.19	1.89	<0.63	5.42	2.41	3.19
	~16.50	~41.38	~6.75			~0.29	~0.52	~3.16		~35.40	~5.67	~14.24

effects in the η and η' wave functions since even though there might be glueball components within the η and η'; uncertainties caused by them may not be as large as other sources such as the DOZI contributions. In these processes, the EM amplitudes are relatively smaller than the strong ones, but the interferences among those strong transition amplitudes turn out to be sensitive. More delicate treatment for those isospin zero channels are needed in further studies. One notices that the branching ratio fraction R can be reasonably accounted for except for the channels involving η'. This might be an indication that additional mechanisms should be considered.

IV. SUMMARY

By systematically analyzing the transition mechanisms for J/ψ and $\psi' \to VP$, we have shown that the long-distance IML transitions are crucial for our understanding of the long-standing $\rho\pi$ puzzle. Since the mass of ψ' is close to the open charm threshold, its decays into VP are affected significantly via the IML transitions. In particular, the long-distance IML transitions provide a mechanism to evade the pQCD HSR and their destructive interferences with the short-distance amplitudes in the ψ' decays cause apparent deviations from the 12% rule. The IML transition turns out to be a rather general nonperturbative mechanism in the charmonium energy region. Our analysis suggests that this mechanism should be present in all the decay modes. The same coincident cancellation between the short- and long-distance amplitudes also causes large charge asymmetries between $\psi' \to K^{*+}K^- + c.c.$ and $K^{*0}\bar{K}^0 + c.c.$

It should be addressed that the open charm threshold effects via the IMLs can also contribute to the process of $\psi(3770) \to VP$. As shown in Refs. [24,39], the IML mechanism can be a natural explanation for the sizeable $\psi(3770)$ non-$D\bar{D}$ decay branching ratios observed in experiment [40–44].

As a manifestation of the open charm threshold effects, the IML mechanism may also play an important role in other decay modes, such as $J/\psi(\psi') \to VS$, VT, PP, etc. As the spin partners of $J/\psi(\psi')$, the study of the ratio of $\mathrm{BR}(\eta_c' \to VV)/\mathrm{BR}(\eta_c \to VV)$ should also be useful for clarifying the role played by the IML and provide some insights into the long-standing $\rho\pi$ puzzle. Such a process has been investigated in Ref. [25] and recently updated in Ref. [26]. We expect that with the help of precise measurements of various decay modes at BESIII, the IML mechanism can be established as an important nonperturbative dynamics in the charmonium energy region.

ACKNOWLEDGMENTS

The authors would like to thank Professors S. Brodsky, K.-T. Chao, C.-H. Chang, T. Huang, X.-Q. Li, and C.-Z. Yuan for useful discussions on this topic. This work is supported, in part, by the National Natural Science Foundation of China Grant No. 11035006, the Chinese Academy of Sciences Grant No. KJCX2-EW-N01, and the Ministry of Science and Technology of China Grant No. 2009CB825200.

[1] A. Duncan and A. H. Mueller, Phys. Lett. B **93**, 119 (1980).
[2] S. J. Brodsky and G. P. Lepage, Phys. Rev. D **24**, 2848 (1981).
[3] V. L. Chernyak and A. R. Zhitnitsky, Nucl. Phys. **B201**, 492 (1982).
[4] K. Nakamura *et al.* (Particle Data Group), J. Phys. G **37**, 075021 (2010).
[5] D. M. Asner *et al.*, in Special issue on Physics at BES-III, edited by K.-T. Chao and Y. Wang [Int. J. Mod. Phys. A 24, 499 (2009)].
[6] Y.-Q. Chen and E. Braaten, Phys. Rev. Lett. **80**, 5060 (1998).
[7] L. J. Clavelli and G. W. Intemann, Phys. Rev. D **28**, 2767 (1983).
[8] S. S. Pinsky, Phys. Lett. B **236**, 479 (1990).
[9] X.-Q. Li, D. V. Bugg, and B.-S. Zou, Phys. Rev. D **55**, 1421 (1997).
[10] M. Suzuki, Phys. Rev. D **57**, 5717 (1998).
[11] C.-T. Chan and W.-S. Hou, Nucl. Phys. **A675**, 367 (2000).
[12] Y. F. Gu and S. F. Tuan, Nucl. Phys. **A675**, 404 (2000).
[13] S. J. Brodsky and M. Karliner, Phys. Rev. Lett. **78**, 4682 (1997).
[14] T. Feldmann and P. Kroll, Phys. Rev. D **62**, 074006 (2000).
[15] J. M. Gerard and J. Weyers, Phys. Lett. B **462**, 324 (1999).
[16] A. Seiden, H. F. W. Sadrozinski, and H. E. Haber, Phys. Rev. D **38**, 824 (1988).
[17] M. Suzuki, Phys. Rev. D **63**, 054021 (2001).
[18] G. Li, Q. Zhao, and C.-H. Chang, J. Phys. G **35**, 055002 (2008).
[19] Q. Zhao, G. Li, and C.-H. Chang, Phys. Lett. B **645**, 173 (2007).
[20] Q. Zhao, G. Li, and C.-H. Chang, Chinese Phys. C **34**, 1704 (2010).
[21] Q. Zhao, Nucl. Phys. B, Proc. Suppl. **207–208**, 347 (2010).
[22] X.-H. Mo, C.-Z. Yuan, and P. Wang, High Energy Phys. Nucl. Phys. **31**, 686 (2007).
[23] X.-Q. Li, X. Liu, and Z.-T. Wei, Front. Phys. China **4**, 49 (2009).
[24] Y.-J. Zhang, G. Li, and Q. Zhao, Phys. Rev. Lett. **102**, 172001 (2009).

[25] Q. Wang, X.-H. Liu and Q. Zhao, arXiv:1010.1343.
[26] Q. Wang, X. H. Liu, and Q. Zhao, arXiv:1202.3026.
[27] X.-H. Liu and Q. Zhao, J. Phys. G **38**, 035007 (2011).
[28] X.-H. Liu and Q. Zhao, Phys. Rev. D **81**, 014017 (2010).
[29] G. Li and Q. Zhao, Phys. Rev. D **84**, 074005 (2011).
[30] F. E. Close and Q. Zhao, Phys. Rev. D **71**, 094022 (2005).
[31] C. Amsler and F. E. Close, Phys. Rev. D **53**, 295 (1996).
[32] F. E. Close and A. Kirk, Phys. Lett. B **483**, 345 (2000).
[33] Y.-D. Tsai, H.-n. Li, and Q. Zhao, Phys. Rev. D **85**, 034002 (2012).
[34] R. Escribano and J. Nadal, J. High Energy Phys. 05 (2007) 006.
[35] H.-Y. Cheng, H.-n. Li, and K.-F. Liu, Phys. Rev. D **79**, 014024 (2009).
[36] P. Colangelo, F. De Fazio, and T. N. Pham, Phys. Rev. D **69**, 054023 (2004).
[37] R. Casalbuoni, A. Deandrea, N. Di Bartolomeo, R. Gatto, F. Feruglio, and G. Nardulli, Phys. Rep. **281**, 145 (1997).
[38] H.-Y. Cheng, C.-K. Chua, and A. Soni, Phys. Rev. D **71**, 014030 (2005).
[39] X. Liu, B. Zhang, and X.-Q. Li, Phys. Lett. B **675**, 441 (2009).
[40] Q. He *et al.* (CLEO Collaboration), Phys. Rev. Lett. **95**, 121801 (2005); **96**, 199903 (2006).
[41] S. Dobbs *et al.* (CLEO Collaboration), Phys. Rev. D **76**, 112001 (2007).
[42] D. Besson *et al.* (CLEO Collaboration), Phys. Rev. Lett. **96**, 092002 (2006).
[43] M. Ablikim *et al.* (BES Collaboration), Phys. Rev. Lett. **97**, 121801 (2006).
[44] M. Ablikim *et al.* (BES Collaboration), Phys. Lett. B **641**, 145 (2006).